# Mathematical modelling and zeta potential determination in the membrane separation process

D. E. PASCU[a], A. R. MIRON[a] , M. TOTU[b], A. C. NECHIFOR[a], E. EFTIMIE TOTU[a*]
[a]*Faculty of Applied Chemistry and Materials Sciences, Politehnica University of Bucharest, Gheorghe Polizu Street, No.1-7, Bucharest, 011061, Romania*
[b]*Faculty of Mechanical Engineering and Mechatronics, Politehnica University of Bucharest, Splaiul Independentei 313, sector 6, Bucharest, 060042, Romania*

Zeta potential is considered an important and reliable indicator of the membrane's surface, and it is essential for the design and operation of membrane processes. In this work, we studied the effect of zeta potential on removing nitrite and sulphite anions from drinking water [1-2]. As zeta potential is sensitive to small chemical changes occurring at surface, it is suitable for monitoring membrane performance. Because, a direct measurement for it is not possible, zeta potential is establish on experimental basis by help of mathematical model [3-4]. The electroosmotic flow is generated by an electrical field able to displace the charged liquid phase within the double layer. Taking into consideration the separation abilities of the composite membranes, they could be an alternative method for the transport and removal of nitrite and sulphites anions from drinking water that could be achieved by electrokinetic effects generated by the anions from aqueous solutions subjected to an electrical field. The aqueous solution containing these anions is pumped through a microchannel whose lateral surfaces are under the direct action of electrical field acting on solution's anions. For microchannel design and chemical species behavior inside it, COMSOL Multiphysics simulation was applied.

(Received April 15, 2015; accepted June 24, 2015)

*Keywords*: Zeta potential, Nitrite, Sulphite, COMSOL Multiphysics programme

## 1. Introduction

According to the classical electrokinetics theory, whenever a solid is in contact with a liquid there adsorption takes place, an electrical charge at the solid surface occurs. As consequence, the solid phase will be electrically charged and it will form a diffuse layer of charged fluid near the opposite radicals'solid surface. The result is an electrical double layer, called the zeta potential. The potential magnitude reflects the amount of solid adsorbed charges [5-6].

By applying an electrical field across an electrolyte solution, the charged particles are attracted to the electrode of the opposite polarity. Viscous forces acting on the particles tend to oppose the particles'motion. The equilibrium is rapidly established between the viscosity and the attraction forces, showing that the particle moves with a constant speed [7-8]. Zeta potential of any material in aqueous solutions is defined not only by one specific process, but also, as conjugated actions of various processes [1, 5].

Unlike a polar medium (water), most of particles show a definite surface charge as consequence of ionization, ionic adsorption and ionic dissolution. This surface charge influences the arrangement of neighbouring anions of the polar medium. Anions will be either attracted to an opposite sign surface particle or they will be repulsed from a surface being similarlly charged [1-2]. Zeta potential is used in colloidal chemistry for observing the behaviour of dispersive system in liquids.

Due to Brown movement and to the supplementary mixing as a consequence of thermal movements, an electrical double layer is formed. The electrical double layer consists of two parts, i.e: an inner part, which includes adsorbed anions and an external or diffuse part where the anions are arranged under the influence of electrical forces and thermal movements [3-4].

In water treatment, zeta potential measurements allow dosage monitoring, thus being possible to reduce the cost of chemical additives through optimizing the dosage control.

The measurement of zeta potential is a way to shorten stability testing by reducing the number of possible formulations, hence reducing the time and costs of testing as well as improving shelf life. Its measurement brings detailed insight on the causes of dispersion, agregation or flocculation and it allows improving the formulation of dispersions, emulsions and suspensions [5-6]. Zeta potential measurement has important applications in a wide range of industries including ceramics, pharmaceuticals, medicine, mineral processing, electronics and water treatment.

Electroosmotic flow was applied for nitrite and sulphite anions in aqueous solution [9]. The potential applied moves the liquid loaded in the charged double layer from microchannel. Thus, if the aqueous solution of nitrite and sulphite ions is positively charged by applying a force to the aqueous solution, it will cause the solution flow in the given direction of the electrical field, while the

ions present in this solution will migrate in different direction through the microchannel.

The rate gradient is perpendicular to the walls of the microchannel and the two directions OX, OY, determine it. By applying an electrical potential then an increased viscous flow and the aqueous solution transport along to rate gradient's direction will occur [10-11].

In this paper, we used two methods to determine zeta potential: an experimental method using an electrophoretic apparatus and a theoretical method using COMSOL Multiphysics programme. We compared the results and the best method has been chosen for determining zeta potential inside the membrane's pore.

## 2. Experimental

The nitrite anion was determined according to STAS 3048/2-96 and SR ISO 6777/96, and the sulphite anion was determined according to STAS 7661/1989 [12-13].

### 2.1. Materials and methods

For experiments, 3 mM KCl solutions were prepared by dissolving KCl salt (Merck) in deionized water. The 0.50 mM, 1.0 mM, and 2.0 mM KCl solutions were prepared by diluting the 3 mM KCl solutions accordingly. The physico-chemical properties of all solutions were measured by help of a *p*H meter (ProfilLine pH 3110) and a conductivity meter (CDM 2d no. 10201). The measured conductivities for 0.50 mM, 1.0 mM, and 2.0 mM KCl solutions were as follows: 105.2 μS/cm, 134.2 μS/cm and 145.1 μS/cm, respectively. The measured *p*H for all solutions was 4.5.

In the current monitoring technique applied to determine the zeta potential of microchannel is implied an electroosmotic flow that involves one fluid which displaces another fluid.

## 3. Results and discussions

The system consists of a microchannels network where the fluid flow is controlled by the electroosmotic effect.

Zeta potential cannot be measured directly, determined from experiments using a mathematical model. The ability to establish the most appropriate math model and to perform the zeta potential measurements for membrane porosity allows measuring the electrolytic conductivity inside the pores of a membrane.

For this purpose, the experimental measurements of the electrical resistance in the pores of the membrane are carried out at different pHs and concentrations. In the present study, there was used as electrolyte 0.50 mM, 1.0 mM, and 2.0 mM KCl to adjust the ionic strength of the solution.

At high pH values, several factors contribute to the negative charge of the membrane surface. The negative surface charge could result from adsorbed anions ($Cl^-$ and $OH_3^+$ from solution). The preferential adsorption of anions has been used to explain the surface charge behaviour for several non-ionogenic surfaces (i.e., surfaces with no ionizable functional groups).

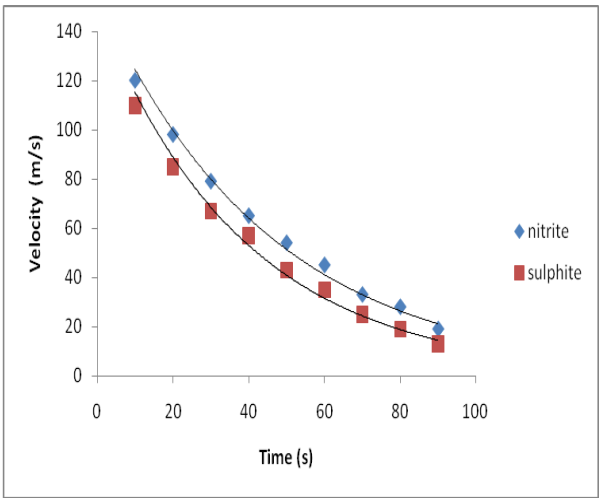


*Fig. 1. Flow rate versus time for nitrite and sulphite ions*

In order to highlight the influence of the electrical potential on the flow rate it was followed the flow rate versus time, figure 1.

By applying an electrical potential to the microchannel's aqueous solution there have been noticed that nitrite anions have showed a higher value of the flow rate than the sulphate anions due to their electrical load. As the conductivity of solutions of nitrite and sulphite anions increases, the flow rate decreases.

### 3.1 The adsorption of nitrite and sulphite ions

*Effect of initial adsorbate concentration:* The adsorption capacities are ranging from 1 to 10 mg $L^{-1}$. The results presented in figure 2 show that higher adsorbate concentration than lower adsorbed amount have been recorded. Such behavior could be assigned to a greater competition for adsorption sites on the adsorbent's surface because more nitrite molecules would be involved. The same pattern was followed by sulphite, except that the decrease in adsorption was progressive and without a maximum as in the case of nitrite. Initial concentration of sulphite and nitrite anions was 10 ppm, and it did not vary over the entire experiment.

In figure 3 is presented the effect of initial concentrations of nitrite and sulphite ions and the influence of pH on the adsorption of sulphite and nitrite ions. These two parameters, namely initial concentration and pH value, affected the adsorption capacity of the membrane. The experimental measurements of zeta potential in pores were performed with the membrane filled with different concentrations of KCl solutions and at

various pH (the farther the pH is from the isoelectric point).

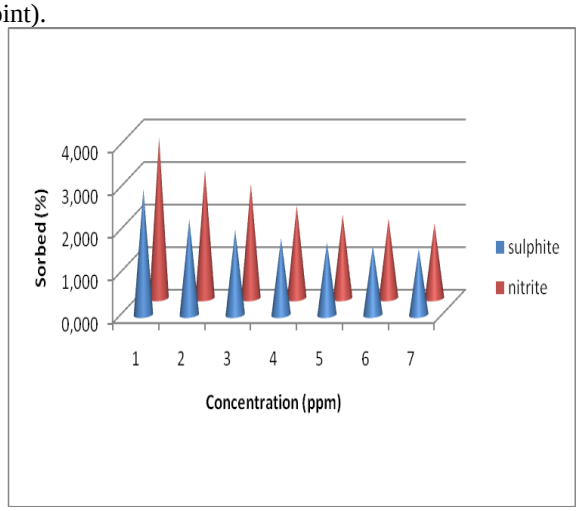


*Fig. 2. Effect of initial concentrations of nitrite and sulphite ions on anions absorption (contact time 45 min, concentration 2.5 ppm)*

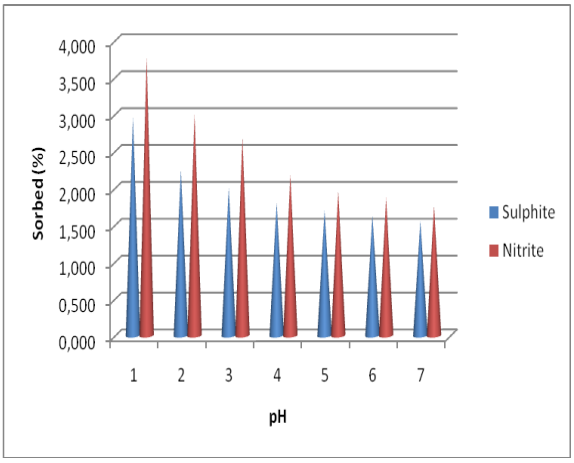


*Fig. 3. Influence of pH on the adsorption of sulphite and nitrite anions*

From the surface conduction experiments it came out that the higher the ratio of the electrolyte conductivity inside pores to the bulk conductivity is, the lower the salt concentration is. It is well known that the surface conduction affects the electrokinetic phenomena [2, 9]. Zeta potential is related to the membrane by the pore conductivity via a space charge model. The simple and fast procedure for determining the zeta potentials for porous membrane is based on the conductivity method. As the values of pH increases, the electrical potential decreases and the flow rate increases.

The adsorption studies have been performed in order to put in evidence the influence of conductivity and zeta potential on the entire system. It has been showed that in any conditions (different pH, high conductivity and high zeta potential), the system behaves in a similar manner and the membrane has the ability of adsorbing the nitrite and sulphite anions.

Zeta potential value has been calculated applying the Smoluchovski equation, presented in a previous article [5]. The flow rate is influenced by the electrical potential. As the electrical potential increases, the flow rate is higher and zeta potential decreases.

The measured zeta potential reflects the dispersion degree of nitrite and sulphite anions inside the microchannel. Nitrite and sulphite anions are partially adsorbed on the membrane surface. The zeta potential has been used to predict the system's stability.

### 3.2 Modelling

The geometry considered in this model is presented in figure 4. In this case, the model involves a T- shaped microchannel of length L = 12 mm, and it is provided on its surface with an active area, namely a composite membrane.

This microchannel consists of two channels:

- (1) one main horizontal channel, and
- (2) a secondary vertical channel.

Also, it has three regions, two for the input and one for the output of the microchannel fluid, numbered from left to right: (1) = outlet region, (2) = inlet region and (3) = inlet region.

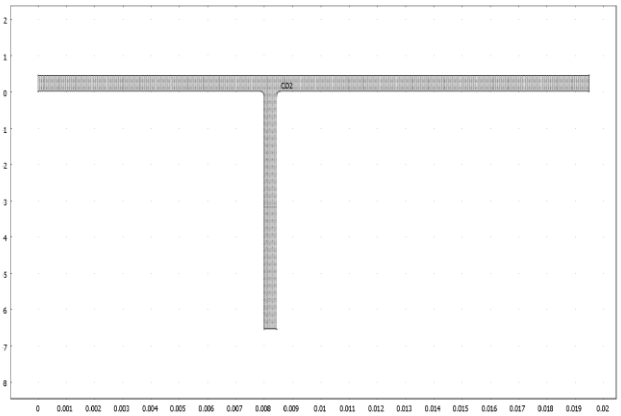

*Fig. 4. The considered system geometry*

### 3.3 Numerical solution

In our work, a 2D finite element model was developed for the simulation of an electroosmotic flow in rectangular channels, and numerical studies were performed using Comsol Multiphysics [14, 21]. Calculations have been carried out according to the following stages: solving the arising potential distribution; then, these distributions were inserted in the Navier-Stokes equation for the calculation of the rate profile.

The values of the zeta potential were in the range 0.15 V and - 40 V. Within mentioned range, the system behaved differently.

Due to electroosmotic effect previously described and depending on the applied potential differences in the

considered microchannel it occurs a flow. The simulation of the flow type is based on the following equations: equation Navier-Stokes for the solution flow through the microchannel [15-16, 19, 22, 23] and the Brinkman equations for the solution's flow through membrane's pores [17-18, 20].
The above-mentioned equations applied for the considered model are:

- The Navier-Stokes equation which describes the flow solution for the microchannel:

$$\nabla[-\eta(\nabla u+(\nabla u)^T+pI)]=-\delta(u\cdot\nabla)\cdot u \qquad (1)$$

and

- The Brinkman equation used for the solution flow within the porous field:

$$\nabla[-\frac{\eta}{\varepsilon_p}(\nabla u+(\nabla u)^T)+pI)]=-\frac{\eta}{k}\cdot u$$

$$\nabla u=0 \qquad (2)$$

where:

- $\delta$ flow's density [kg/m$^3$];
- u rate [m/s];
- $\eta$ dinamic viscozity [Pa · s];
- p flow's preasure [Pa];
- T tensions' tensor;
- $\nabla$ the spatial derivation operator;
- K permeability fluid's [m$^2$];
- $\varepsilon_p$ membrane's porosity.

The results of numerical simulations carried out in this work are presented in the figures 5 to 8, from where the typical data for the solution/fluid velocity when the electrical potential distributions have been obtained under the boundary conditions of the process could be follow-up. The system functioning is based on the electrical potential distribution inside the microchannel (see figure 9).

In figure 5, one can observe that at different potentials the average rate in microchannel was about 0.1 m/s. From the plot it comes out that the highest rate was recorded at the corners' wall junction of the microchannel (whose geometry is as T form), where the electrical field is high, while the rate on solid surfaces is zero at normal pressure flow of aqueous solution.

In this particular case, we consider that the aqueous solution is flowing through the main channel 1 horizontally (avoiding secondary flow), and through channel 2 vertically. This is done by applying an electrical potential as follows: from figure 5 plot - region 1 (output) of the microchannel = 290V, region 2 (input) = 198V, region 3 (input) = 100V and ζ - potential = 0.15V; and from figure 6 plot - region 1 (output) = 290V, region 2 (input) = 198V, region 3 (input) = 100V and ζ - potential = - 40V.

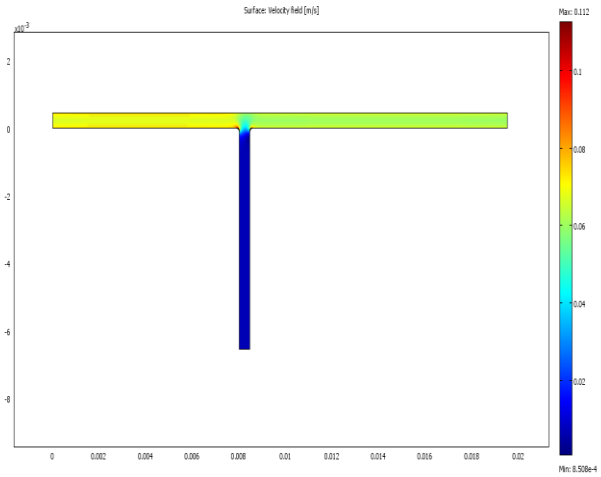

*Fig. 5. Rate distribution in the microchannel, electrical potential applied to region (1) =290V, region (2) =198V, region (3) =100V and ζ - potential = 0.15V*

Fig. 6 presents the rate distribution within the T microchanel along channel 1 horizontally from right to left, the rate of fluid's flow being minimized in the channel bottom. In this case, the highest rate is represented by red color to garnet red in the gate region 3 and 1 (right to left) of the microchannel (along OX axis). The maximum values of the rate tends to increase towards the gate 1 (output), unlike the previous example, due to the change in the zeta potential ζ-region (1) from 0.15V to - 40V, which means that the entire process is stable.

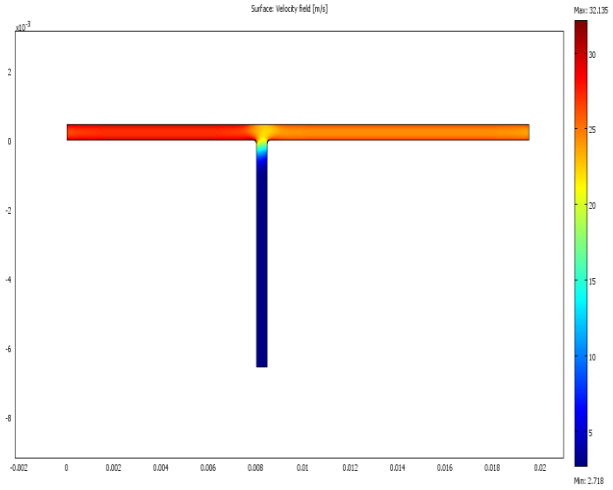

*Fig. 6. Rate distribution in the microchannel, electrical potential applied to region 1(outlet) =290V, region 2 (inlet) =198V, region 3(inlet) =100V and ζ - potential = - 40V.*

At this stage, we implemented the following potential electronic distribution: region 1(outlet) =100V, region 2(inlet) = 0V, region 3(inlet) = 0V and ζ - potential = 0.15V (figure 7). The maximum value of the flow was obtained on the left side of the corner of the walls of the microchannel junction and the flow of the aqueous solution in this case took place from left bottom channel to the left channel with ζ -potential = 0.15V. The electrical potential can efficiently change the flow path in the channels.

Fig. 7 presents a different direction of the solution flow due to the electrical potential applied to the input and output regions of the microchannel, unlike the flow solution presented in fig. 6, where zeta potential had a lower value.

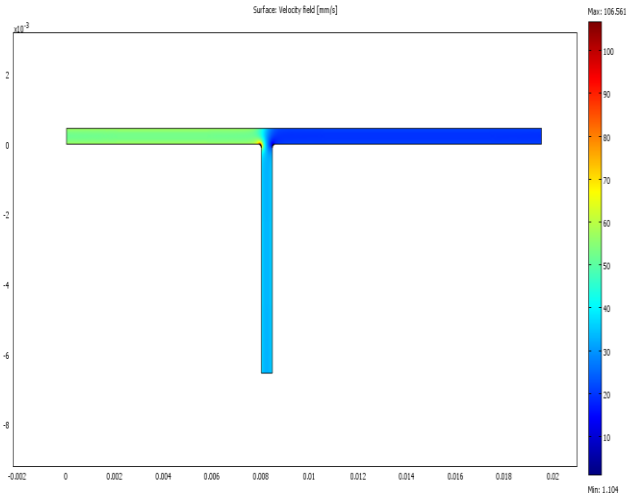


*Fig. 7. Rate distribution in the microchannel, electrical potential applied to region 1(outlet) =100V, region 2 (inlet) = 0V, region 3(inlet) = 0V and ζ - potential = 0.15V*

In figure 8, there could be seen that the flow decreases in the outer parts of the microchannel, while a maximum flow occurs in the inner parts thereof. From this plot, it could be seen that the rate is at its maximum, its value being much higher than in the previous case. This could be assigned to the fact that the electrical field is much stronger around junction's corners of the microchannel compared to the straight path of fluid flow. This case is similar to the previous simulation case, presented in figure 7, but with specific modeling applied on the microchannel's surface at ζ -potential = - 40V.

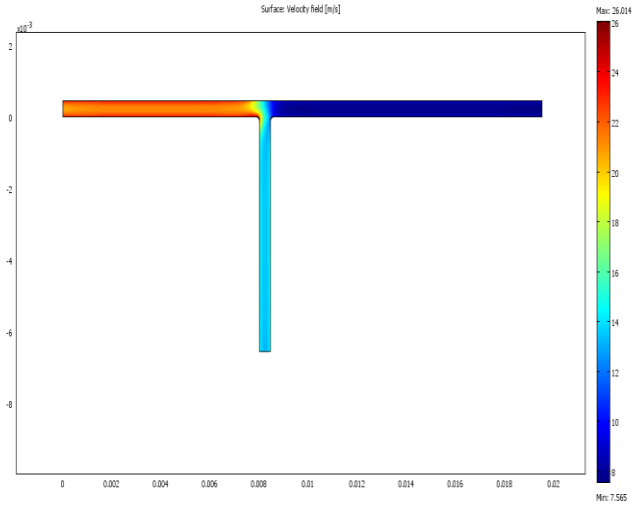


*Fig. 8. Rate distribution in the microchannel, electrical potential applied region 1(outlet) =100V, region 2 (inlet) = 0V, region 3(inlet) = 0V and ζ - potential = - 40V*

While the rate distribution could be follow-up in figures 5 to 8, figures 6 to 8 show the temporal evolution of the solution's rate field. The time considered for the simulation ranged between 0 - initial step, (figure 5) and 1.307 s (figure 8).

The distribution of the electrical potential applied to the channel is shown in figure 9 (a, b). From this distribution graph, it could be observed an alternation between the minimum and the maximum of the electrical potential distribution within five significant areas. The red garnet color corresponds to the maximum electric potential.

The largest electrical potential differences occurred on the horizontal direction, implying that the flow of the solution was in the same direction for the first two simulations, while for the last two simulations the flow of the solution was from bottom to the left hand of the main channel.

The reduced deviation at the crossing junction (at the intersection of the secondary channel (2), with the main channel (1)) of the T microchannel for aqueous solution flow could be follow-up by help of the rate flow lines along the microchannel - see figure 10.

The plot from figure 10 uses intense blue color for velocity, characterizing the fall in the middle section connecting the junction's corners of the secondary channel (2) of the system.

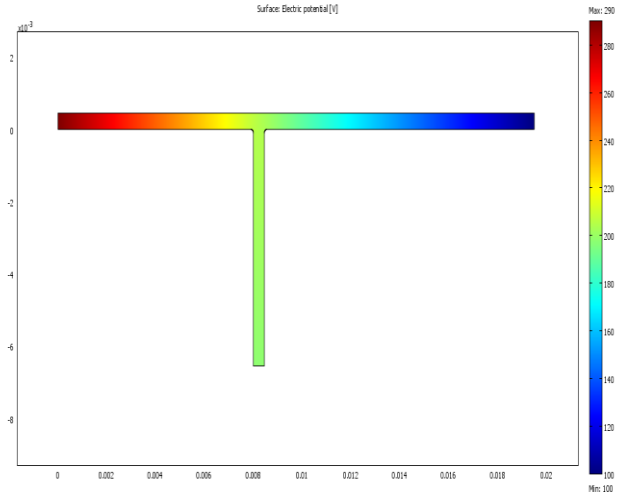

*(a) region 1(inlet) electrical potential = 290V, region 2(inlet) = 198V, region 3(inlet) = 100V*

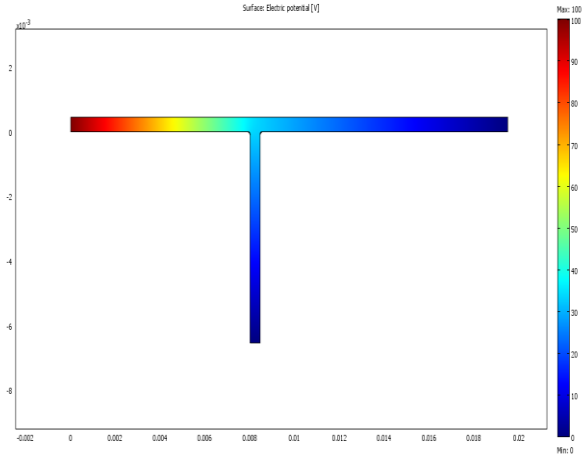

*(b) region 1(inlet) electrical potential=100V, region 2(inlet) = 0V, region 3(inlet) = 0V*

*Fig. 9. Electrical potential distribution in the microchnnel*

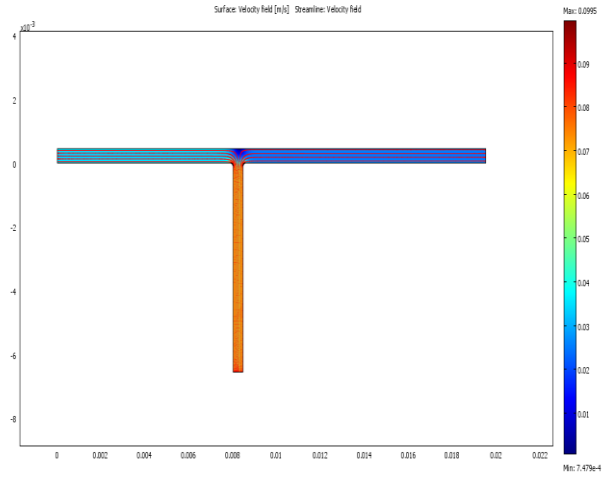

*Fig. 10. Velocity streamline in the microchannel.*

The membrane's zeta potential is related to the electrolyte conductivity inside the pores, because the mobility of ions and their concentration are controlling the conductivity.

When a membrane gets into contact with an aqueous solution, its surface acquires a characteristic electrical surface area. In order to mantain the electroneutrality of the system, the ions' charges within the adjacent solution are reorganized.

At the surface of the membrane there has been formed an electrical "double layer", and zeta potential varied progressively from the charged surface to the bulk solution. The conductivity inside the pores may significantly exceed the conductivity of the bulk solution, because of the counter anions excess in the adjacent solution.

The determined numerical values of zeta potential differ from one method to another. The reproducibility of the results for both methods is better than the differences observed, confirming that the precision of the measurements is not the cause of these differences.

It was observed that the experimental method gives values of the zeta potential lower than those calculated with the COMSOL programme. The zeta potential increases as the pH vary from 1 to 10, as it would be expected for a surface with acid-base groups.

## 4. Conclusions

An important part of the investigations over zeta–potentials is based on the presumption that there is an interacting dependence between the zeta – potential and the sulphite and nitrite anions, which are present in drinking water in various concentrations.

In this study, there have been measured the streaming potentials and the electrolyte conductivities inside the pores over a pH range and at a certain ionic strength (adding KCl as support electrolyte).

The pore conductivity measurements and the flow rate could be used to determine the zeta potentials of the porous membrane and the results obtained are presented in the present work.

From the performed experiments it came out that higher the ratio of the electrolyte conductivity inside pores to the bulk conductivity is lower the salt concentration is. In addition, it has been observed that the increasing values for pH and flow rate are related to the electrical potential decreasing values.

A 2D finite element model is developed for the simulation of an electroosmotic flow in rectangular channels, and numerical studies were performed using Comsol Multiphysics.

The electrical potential can efficiently change the flow path in the channels. The membrane's zeta potential is related to the electrolyte conductivity inside the pores.

For calculations have been applied the Navier-Stokes and Brinkman equations for the flow solution in microchannel and for the porous field, respectively.

The experiments proved that the average flow rate in the microchannel was 0.1 m/s at various potentials, and the highest flow rate was recorded at the corners' wall junction of the microchannel (with T geometry).

The entire process is stable when the maximum values of the flow rate tends to increase towards the region 1(output), due to the change of zeta potential (ζ) from 0.15V to - 40V.

It has been demonstrated that in any conditions (various pHs, conductivity and zeta potential with high values), the system behaves similarly and the membrane has the ability of adsorbing the nitrite and sulphite anions.

The method for estimating the zeta potentials for porous membrane using COMSOL Multiphysics programme has the advantage of being a simple and fast procedure. This method proved to be an attractive method for characterizing small pores or large pores with strongly charged surfaces.

**Acknowledgements**

The work has been funded by the Sectorial Operational Programme Human Resources Development 2007-2013 of the Ministry of European Funds through the following Financial Agreements: POSDRU/159/1.5/S/132395, POSDRU/159/1.5/S/134398 and POSDRU/159/1.5/S/137070.

Faculty of Applied Chemistry and Materials Sciences, Politehnica University of Bucharest, support is also gratefully acknowledged.

## References

[1] Gh. Nechifor, D. E. Pascu, M. Pascu (Neagu), V. I. Foamete(Panait) U.P.B. Sci. Bull. **75**, 191 (2013).
[2] P. Fievet, A. Szymczyk, C. Labbez, B. Aoubiza, C. Simon, A. Foissy, and J. Pagetti, J COLLOID INTERFACE SCI, **235**, 383 (2001).
[3] S. Honorary and F. Zahir - A Review (Part 1), Trop J Pharm Res., **12**(2), 255 (2013).
[4] A. N. D. Lawrence, J. M. Perera, M. Iyer, M. W. Hickey, G.W. Stevens, Sep Purif Techno, **48**(2), 106 (2006).
[5] Gh. Nechifor, D.E. Pascu, M. Pascu (Neagu), G. A. Traistaru , A. A. Bunaciu and H. Y. Aboul-Enein, Rev. Roum. Chim. **58**(7-8), 591 (2013).
[6] A. Jang, Y. Seo, P. L Bishop, Environmental Pollution, **133**, 117 (2005).
[7] A. P. Davis, M. Shokouhian, H. Sharma, and C. Minami, Water Environment Research, **78**(3), 284 (2006).
[8] M. Kanematsu, A. Hayashi , M. S. Denison, T. M. Young, Chemosphere, **76**(7), 952 (2009).
[9] Z. Zheng, J. Derek, Hansford, and A. T. Conlisk, Electrophoresis, **24**, 3006 (2003).
[10] Guidelines for drinking-water quality, 2nd ed, vol.2, Health criteria and other supporting information, Geneva, World health organization, 1996,p.940–949 and Addendum 2 , 1998, p. 281–283.
[11] S. Salgın, U. Salgın and N. Soyer, Int. J. Electrochem. Sci. **8**, 4073 (2013).
[12] Nitrite anion determination from potable water according STAS 3048/2-96 and SR ISO 6777/96.
[13] Sulphite anion determination from potable water according STAS 7661/1989.
[14] Comsol Documentation, "Chemical Engineering Module User's Guide", Comsol **AB**, (2008).
[15] P.M. Gresho and R.L. Sani, Incompressible Flow and the Finite Element Method, Volume 2: Isothermal Laminar Flow, John Wiley and Sons, LTD, (2000).
[16] D.J. Tritton, Physical Fluid Dynamics, 2nd ed., Oxford University Press, (1988).
[17] G.F. Froment, K.B. Bischoff, Chemical Reactor Analysis and Design, 2nd ed., John Wiley & Sons, (1990).
[18] C.W. Spalding, AIChE J. , **8**(5), 685 (1962).
[19] G.K. Batchelor, Cambridge University Press, (1967).
[20] C. Johnson, Numerical solution of partial differential equations by the finite element method, Student litteratur, (1987).
[21] F. A. Guarnieri, P. A. Kler and C. L. A. Berli, Mecánica Computacional Vol **XXV**, 2573 (2006).
[22] M. Zoran, R. Savastru, D. Savastru, M. N. M. Tautan, S. I. Miclos, D. C. Dumitrasa, T. Julea, Journal of Optoelectronics and Advanced Materials, **12**(1), 159 (2010).
[23] M.-R. Ioan, I. Gruia, P. Ioan, M. Bacalaum, G–V. Ioan, C. Gavrila, Journal of Optoelectronics and Advanced Materials, **15**(5 – 6), 523 (2013).

*Corresponding author: eugenia_totu@yahoo.com